COHERENT constraint on leptophobic dark matter using CsI data

D. Akimov,[1] P. An,[2,3] C. Awe,[2,3] P. S. Barbeau,[2,3] B. Becker,[4] V. Belov,[5,1] I. Bernardi,[4] M. A. Blackston,[6] C. Bock,[7] A. Bolozdynya,[1] R. Bouabid,[2,3] J. Browning,[8] B. Cabrera-Palmer,[9] D. Chernyak,[7,a] E. Conley,[2] J. Daughhetee,[6] J. Detwiler,[10] K. Ding,[7] M. R. Durand,[10] Y. Efremenko,[4,6] S. R. Elliott,[11] L. Fabris,[6] M. Febbraro,[6] A. Gallo Rosso,[12] A. Galindo-Uribarri,[6,4] M. P. Green,[3,6,8] M. R. Heath,[6] S. Hedges,[2,3] D. Hoang,[13] M. Hughes,[14] B. A. Johnson,[14] T. Johnson,[2,3] A. Khromov,[1] A. Konovalov,[1] E. Kozlova,[1,5] A. Kumpan,[1] L. Li,[2,3] J. M. Link,[15] J. Liu,[7] A. Major,[2] K. Mann,[8] D. M. Markoff,[16,3] J. Mastroberti,[14] J. Mattingly,[17] P. E. Mueller,[6] J. Newby,[6] D. S. Parno,[13] S. I. Penttila,[6] D. Pershey,[2,*] C. Prior,[2,3] R. Rapp,[13] H. Ray,[18] O. Razuvaeva,[1,5] D. Reyna,[9] G. C. Rich,[3] J. Ross,[16,3] D. Rudik,[1] J. Runge,[2,3] D. J. Salvat,[14] A. M. Salyapongse,[13] J. Sander,[7] K. Scholberg,[2] A. Shakirov,[1] G. Simakov,[1,5] W. M. Snow,[14] V. Sosnovstsev,[1] B. Suh,[14] R. Tayloe,[14] K. Tellez-Giron-Flores,[15] I. Tolstukhin,[14,b] E. Ujah,[16,3] J. Vanderwerp,[14] R. L. Varner,[6] C. J. Virtue,[12] G. Visser,[14] T. Wongjirad,[19] Y.-R. Yen,[13] J. Yoo,[20] C.-H. Yu,[6] and J. Zettlemoyer[14,c]

[1]*National Research Nuclear University MEPhI (Moscow Engineering Physics Institute), Moscow 115409, Russian Federation*
[2]*Department of Physics, Duke University, Durham, North Carolina 27708, USA*
[3]*Triangle Universities Nuclear Laboratory, Durham, North Carolina 27708, USA*
[4]*Department of Physics and Astronomy, University of Tennessee, Knoxville, Tennessee 37996, USA*
[5]*National Research Center "Kurchatov Institute" Kurchatov Complex for Theoretical and Experimental Physics, Moscow 117218, Russian Federation*
[6]*Oak Ridge National Laboratory, Oak Ridge, Tennessee 37831, USA*
[7]*Physics Department, University of South Dakota, Vermillion, South Dakota 57069, USA*
[8]*Department of Physics, North Carolina State University, Raleigh, North Carolina 27695, USA*
[9]*Sandia National Laboratories, Livermore, California 94550, USA*
[10]*Center for Experimental Nuclear Physics and Astrophysics and Department of Physics, University of Washington, Seattle, Washington 98195, USA*
[11]*Los Alamos National Laboratory, Los Alamos, New Mexico 87545, USA*
[12]*Department of Physics, Laurentian University, Sudbury, Ontario P3E 2C6, Canada*
[13]*Department of Physics, Carnegie Mellon University, Pittsburgh, Pennsylvania 15213, USA*
[14]*Department of Physics, Indiana University, Bloomington, Indiana 47405, USA*
[15]*Center for Neutrino Physics, Virginia Tech, Blacksburg, Virginia 24061, USA*
[16]*Department of Mathematics and Physics, North Carolina Central University, Durham, North Carolina 27707, USA*
[17]*Department of Nuclear Engineering, North Carolina State University, Raleigh, North Carolina 27695, USA*
[18]*Department of Physics, University of Florida, Gainesville, Florida 32611, USA*
[19]*Department of Physics and Astronomy, Tufts University, Medford, Massachusetts 02155, USA*
[20]*Department of Physics and Astronomy, Seoul National University, Seoul 08826, Korea*

(Received 26 May 2022; accepted 30 August 2022; published 14 September 2022)

We use data from the COHERENT CsI[Na] scintillation detector to constrain sub-GeV leptophobic dark matter models. This detector was built to observe low-energy nuclear recoils from coherent elastic neutrino-nucleus scattering. These capabilities enable searches for dark matter particles produced at the Spallation Neutron Source mediated by a vector portal particle with masses between 2 and 400 MeV/c^2. No evidence for dark matter is observed and a limit on the mediator coupling to quarks is placed. This constraint improves upon previous results by two orders of magnitude. This newly explored parameter space probes

*daniel.pershey@duke.edu
[a]Present address: Department of Physics and Astronomy, Tuscaloosa and Institute for Nuclear Research of NASU, Kyiv 03028, Ukraine.
[b]Present address: Argonne National Laboratory, Argonne, Illinois 60439, USA.
[c]Present address: Fermi National Accelerator Laboratory, Batavia, Illinois 60510, USA.

the region where the dark matter relic abundance is explained by leptophobic dark matter when the mediator mass is roughly twice the dark matter mass. COHERENT sets the best constraint on leptophobic dark matter at these masses.

DOI: 10.1103/PhysRevD.106.052004

I. INTRODUCTION

There is overwhelming evidence for the gravitational effects of dark matter which comprises ≈80% of the matter in the Universe [1]. Despite several experimental techniques developed to detect dark matter, its particle nature is still not understood. To resolve this question, several experimental approaches have been attempted to identify dark-matter particles using both astroparticle [2–4] and accelerator-based techniques [5,6].

COHERENT detectors deployed at the Spallation Neutron Source (SNS) are sensitive to dark-matter particles produced in the target with masses below the current beam energy, ≈1 GeV. From cosmological constraints, sub-GeV dark matter cannot interact directly with standard-model particles through the weak force [7]. Instead, light dark matter would consist of hidden sector particles, χ, whose interactions with standard-model particles are mediated by a vector portal particle V. Sub-GeV dark matter may be scalar or fermionic, and there are different channels through which V could interact with standard-model particles.

Detectors sensitive to low-energy nuclear recoils induced by coherent elastic neutrino nucleus scattering (CEvNS) are efficient probes of light dark matter with masses below ≈1 GeV. These detectors would also observe nuclear recoils induced by coherent χ-nucleus scattering if dark matter is produced at the SNS. The cross section for this process is proportional to the square of the nucleon number, A [8] so that a small detector can yield a result competitive with constraints from much larger detectors that rely on inelastic signal channels. Additionally, as accelerator-produced light dark matter is relativistic, the scattering cross section is relatively independent of dark matter spin [9] so that CEvNS detectors can effectively search for both scalar and fermionic dark matter.

II. COHERENT AT THE SNS

The COHERENT collaboration employs several detectors at the SNS at Oak Ridge National Laboratory [10]. We measure CEvNS and other low-energy scattering processes on several types of nuclei and maintain neutron detectors to understand beam-related backgrounds. Detectors are placed in a basement hallway, Neutrino Alley, where neutron backgrounds are low enough to permit these measurements of low-energy scattering processes about 20 m from the SNS target. The SNS is a π decay-at-rest (π-DAR) source with a FWHM beam pulse width of 360 ns offering a prompt ν_μ flux and delayed $\nu_e/\bar{\nu}_\mu$ flux separated in time. Having multiple flavors and separation by timing is ideal for testing beyond-the-standard-model (BSM) scenarios such as lepton flavor universality of the CEvNS cross section (at tree level) and for searches for hidden sector particles such as dark matter.

To study CEvNS, we have built several detectors sensitive to low-energy nuclear recoils. The COHERENT CsI[Na] detector was a 14.6 kg, low-background scintillating crystal commissioned at the SNS which made the first observation of CEvNS in 2017 [11]. Scintillation light was collected by a single Hamamatsu R877-100 photomultiplier. Neutron and γ backgrounds were mitigated by a composite shielding using both low-activity lead and low-Z materials. The assembly was surrounded by a plastic scintillator veto to reject cosmic-induced activity. The detector collected beam data from 2017 to 2019, recording a total of 3.20×10^{23} protons-on-target during its run. Recently, the full dataset from the detector, along with improved understanding of the detector response to nuclear recoils, enabled the most precise measurement of the CEvNS cross section yet [12] and placed leading constraints on sub-GeV dark matter [13].

Additionally, we study CEvNS on Ar with continuing operation of a liquid argon scintillation detector. This detector made the first measurement of the CEvNS cross section on Ar [14] with an active argon mass of 24 kg. COHERENT is also currently commissioning low-threshold CEvNS detectors with Ge and Na targets along with a heavy-water Cherenkov detector to calibrate the neutrino flux at the SNS [15]. Neutron detectors are currently running to monitor beam-related backgrounds [16]. COHERENT also plans for future large-scale detectors which will dramatically improve precision of measurements on small, first-light detectors [17].

III. LEPTOPHOBIC DARK MATTER

COHERENT has previously reported a dark-matter constraint using these data on a model that predicts a vector portal particle V that kinetically mixes with the photon and decays to dark-matter particles χ [13]. A leptophobic, or baryonic, dark-matter model [18–23] is also viable where V mediates interactions between χ and quarks described in terms of the vector mediator, V^μ, and the scalar dark matter particle, χ, by Lagrangian terms

$$\mathcal{L} \supset -g_B V^\mu J^B_\mu + g_\chi V^\mu (\partial_\mu \bar{\chi}\chi - \bar{\chi}\partial_\mu \chi), \tag{1}$$

where J^B_μ is the baryon current given by

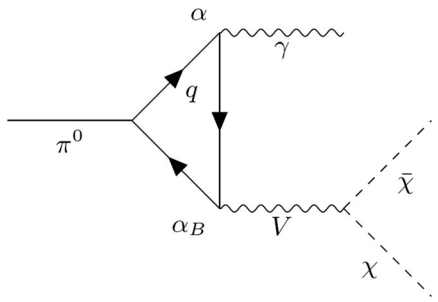

FIG. 1. Production of leptophobic dark matter from π^0 decay which may occur at the SNS. The dark matter particles are on-shell and may subsequently scatter coherently in a COHERENT detector.

$$J_\mu^B = \frac{1}{3}\sum_q \bar{q}\,\gamma_\mu q. \tag{2}$$

This implies the couplings $\alpha_B \equiv g_B^2/4\pi$ and $\alpha_\chi \equiv g_\chi^2/4\pi$ describing Vqq and $V\chi\chi$ vertices, respectively. Production of leptophobic dark matter can be achieved in π^0 decay by the diagram shown in Fig. 1 with a branching ratio $\mathrm{Br}(\pi^0 \to \gamma V) \propto 2\alpha_B/\alpha$. Coherent $\chi - A$ scattering off a nucleus, A, occurs through simple V exchange with $\sigma(\chi A \to \chi A) \propto \alpha_B\alpha_\chi$.

Though there is no $V - \gamma$ kinetic mixing in the leptophobic dark matter model at tree level, there is an effective mixing from the loop diagram shown in Fig. 2 with a mixing parameter $\varepsilon \sim e g_B/(4\pi)^2$. Through this effective kinetic mixing, the couplings for leptophobic dark matter can be related to the dark-matter scattering cross section at freeze-out which determines the modern relic abundance.

There are several current constraints on this model from Coherent Captain Mills [6], NA62 [24], MiniBooNE [25,26], and neutron-scattering [27]. There is also a model-dependent anomalon limit considering the influences of dark matter on anomalous SM baryonic couplings [28]. These constraints exclude leptophobic dark matter for all values of α_χ if $m_V/m_\chi > 3$.

However, there is significant parameter space viable for $m_V/m_\chi \approx 2$. If $0 < m_V - 2m_\chi < T_f \approx m_\chi/20$, with T_f the freeze-out temperature, then the annihilation rate of dark matter would have happened on resonance [29] in the early universe during thermal freeze-out, increasing the $\bar{\chi}\chi \to$ SM cross section. For a given m_χ, this resonant enhancement is proportional to $e^{-(m_\chi/T_f)\varepsilon_R}$ where $\varepsilon_R \equiv (m_V^2 - 4m_\chi^2)/4m_\chi^2$ [29]. If $\varepsilon \ll 1$, the resonant condition $m_V - 2m_\chi < T_f$ can be approximated by $\varepsilon < 1/20$. As the annihilation cross section can be determined from the relic dark matter density, this resonance implies that model couplings required to produce the observed relic density are much lower when $\varepsilon < 1/20$. Thus experimental searches for leptophobic dark matter in experiments must probe significantly lower couplings if m_V/m_χ is slightly above 2. Thus, couplings required to match the relic abundance of dark matter also depend on ε_R with decreasing target couplings as $\varepsilon_R \to 0$. For scalar leptophobic dark matter, this effect reaches a floor for $\varepsilon_R < 10^{-5}$ where lower values of ε_R do not further suppress expected dark matter couplings. For fermionic dark matter, however, this effect is unbounded with $\varepsilon_R \to 0$ driving the coupling required to match the relic abundance to arbitrarily low values.

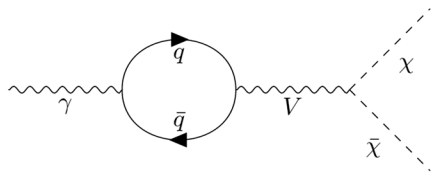

FIG. 2. The $\gamma - V$ kinetic mixing induced from leptophobic dark-matter portal through a virtual quark loop and subsequent $V \to \bar{\chi}\chi$ decay.

The dominant production mechanisms for leptophobic dark matter at the SNS are $\pi^0 \to \gamma V$ and $\eta^0 \to \gamma V$ facilitated through a Vqq vertex for the SNS beam energy as was the case with the leptophilic model [13]. A leptophobic dark matter particle passing through the CsI[Na] detector can scatter coherently with target nuclei, producing a nuclear recoil signature with similar energies to those expected from CEvNS. The differential cross section is given in terms of the nuclear mass, m_N, recoil energy, E_r, nuclear form factor, $F(Q^2)$, and momentum transfer, $Q^2 = 2m_N E_r$ as

$$\frac{d\sigma}{dE_\mathrm{r}} = 4\pi\alpha_B\alpha_\chi A^2 \frac{2m_N E_\chi^2}{p_\chi^2(m_V^2 + Q^2)^2}|F(Q^2)|^2, \tag{3}$$

where p_χ and E_χ are the momentum and energy of the incident dark-matter particle. Timing of the π-DAR beam can differentiate the dark matter signal from CEvNS background as relativistic dark matter [30] produced by decay-in-flight of mesons in the SNS target would arrive coincident with the protons-on-target while the neutrino flux has a prompt ν_μ and delayed $\nu_e/\bar{\nu}_\mu$ flux. Production and scattering rates are predicted by the BdNMC event generator [22].

IV. ANALYSIS AND RESULTS

The COHERENT CsI[Na] detector performance, along with discussion of event selection and background rates are presented here and discussed in detail in [12,13]. Using calibration data from the 59.5-keV γ peak from ^{241}Am, we measured a light yield of 13.35 PE/keV$_{ee}$, or photoelectrons per keV of electronic recoil energy, in the CsI[Na] detector. Nuclear recoil quenching was modeled by a polynomial fit to five neutron scattering measurements using a small CsI[Na] crystal with identical doping [31]. A pulse-finding reconstruction was run on PMT waveforms to calculate a recoil time and energy for each event.

The single photoelectron (SPE) charge was calibrated by taking the average waveform integral of isolated pulses found outside the beam window. For each beam spill, events were selected that have low background scintillation activity within the crystal prior to the beam spill and ≥ 9 reconstructed pulses. Calibration data were taken with a ^{133}Ba γ source which determined the nuclear recoil threshold by observing Compton electrons. Though these are electronic recoils, the scintillation decay time is very similar to that observed for nuclear in CsI[Na] [32].

These requirements resulted in a nuclear recoil threshold of ≈ 9 keV$_{nr}$ which was measured using ^{133}Ba calibration data. A four-parameter function was fit to the ^{133}Ba data and also used to estimate the uncertainty in the threshold, ≈ 1 keV$_{nr}$. The efficiency is shown in Fig. 3 for simulated $m_V = 80$ MeV/c^2 dark matter giving an average selection efficiency of 21% at this mass.

Beam-unrelated backgrounds account for the majority, 78%, of the total background below 60 PE and were measured in-situ with data out of time with the beam. Due to afterglow scintillation activity within the crystal, the selection efficiency depends on recoil time as later recoils may be rejected due to spurious background activity earlier in the waveform. The remaining backgrounds are neutron-related (2%) whose normalizations were determined with data from a liquid scintillator housed in the CsI[Na] shielding collected before commissioning the CEvNS detector and CEvNS events (20%). The total systematic uncertainty on the CEvNS rate was 12% and was dominated by the neutrino flux uncertainty [33] with additional uncertainty calculated for quenching, the detection threshold model, form factor suppression, and background normalizations.

To determine the dark matter content within the observed data, a binned log-likelihood was developed. All selected data with $E_{rec} < 250$ PE and $t_{rec} < 6$ μs were included and fit in two dimensions, recoil energy and time. This fit included both prompt and delayed data. Though no dark matter is expected for $t_{rec} > 6$ μs, these data were included to improve constraints on nuisance parameters. Nine nuisance variables were included to incorporate systematic uncertainties. Four only affected background rate: the neutrino flux uncertainty, the rate of steady-state background, and two for neutron backgrounds. There were also five parameters that affect rate and shape of the prediction of the dark matter signal and backgrounds: the timing of the arrival of the neutrino pulse, the detector threshold, the nuclear form factor, and two covering uncertainty in quenching determined by a principal component analysis. The number of dark matter counts is determined by calculating a profile-log $\mathcal{L}$ curve from observed data. As the expected recoil shape of the dark matter signal depends on m_V, a fit was developed for multiple assumptions on the mediator mass over the tested region.

The observed data were fit with the best-fit spectra shown in Fig. 4. For each dark matter mass tested, the

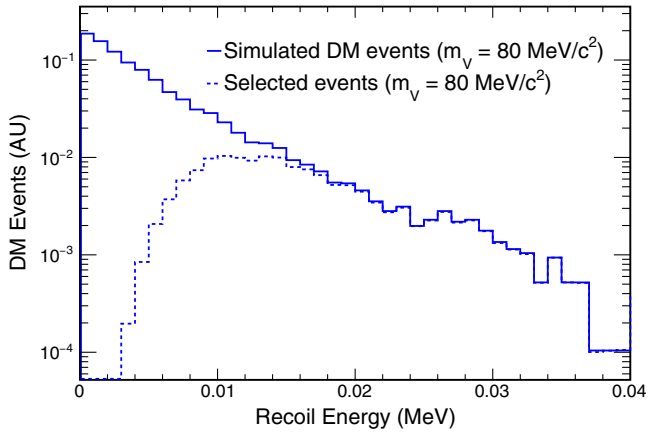

FIG. 3. Selection efficiency for simulated dark matter near the most sensitive mass. With an approximately 9 keV$_{nr}$ threshold, the selection efficiency is 21% for dark matter.

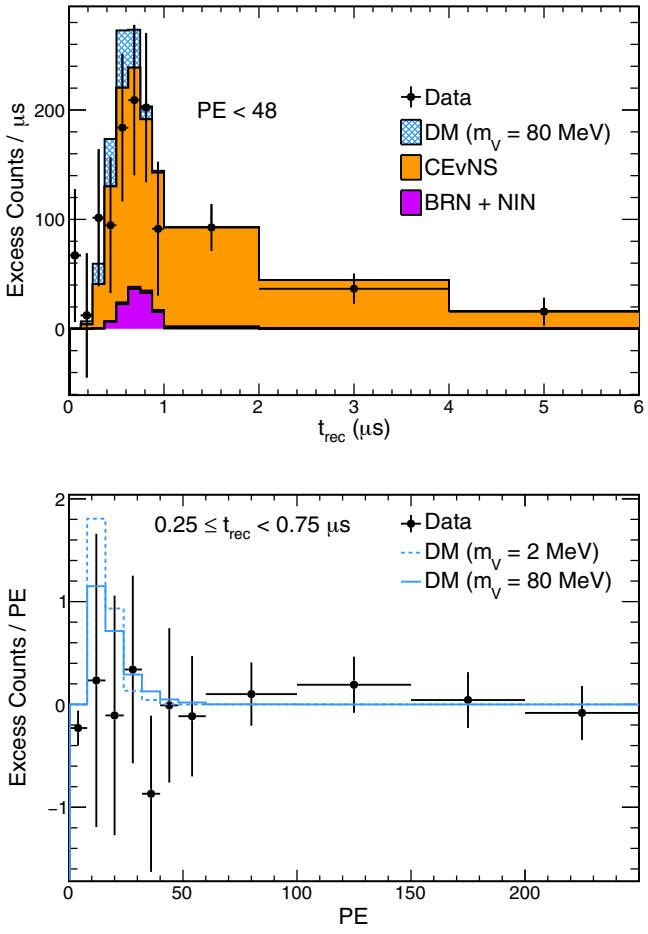

FIG. 4. The timing distribution of the beam-related excess (top) is shown with the 90% confidence level limit on dark matter content stacked with CEvNS and neutron (BRN and NIN) backgrounds at the best fit (with no dark-matter events). The recoil energy distribution, with all backgrounds subtracted (including CEvNS), is also shown (bottom) with two assumptions of mediator mass.

best-fit parameters suggest no dark matter events with a χ^2/dof of 103/120. A clear timing region of interest is identified between 0.25 and 0.75 μs where the majority of dark matter is expected with a background control region at recoil times above 0.75 μs.

COHERENT data test leptophobic dark matter in the most conservative scenarios for $\varepsilon_R > 0$. As such, couplings that match the relic abundance depend strongly on m_V/m_χ. For a fixed m_V, the expected dark-matter distribution does not change with varying m_χ for all $m_\chi < m_V/2$. We thus show results in terms of m_V. For a given value of m_V, α_χ is assumed to be 0.5, as smaller values lead to stronger constraints and the model becomes nonperturbative at higher values. A confidence interval is constructed for α_B using a log-likelihood spectral fit and the Feldman-Cousins method [34] at the 90% confidence level. The resulting contour is shown in Fig. 5 compared to relic abundance targets with different assumptions of ε_R for both scalar and fermionic dark matter. At our strongest constraint, $m_V = 80$ MeV/c^2, the Feldman-Cousins treatment of our fit results suggest < 17 dark matter events in the sample at the 90% confidence level.

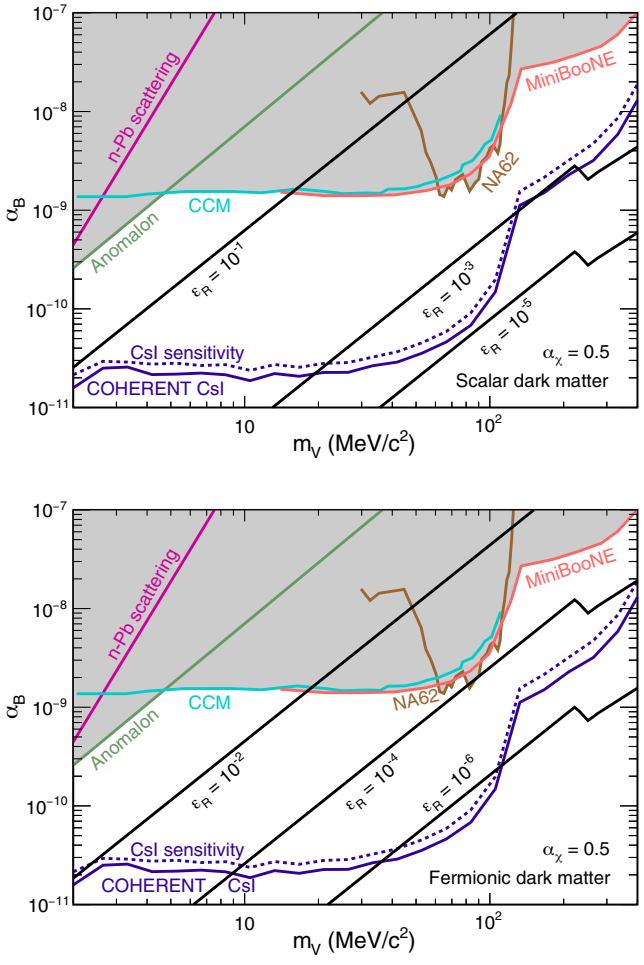

FIG. 5. Constraint on leptophobic parameter space from CsI [Na] data along with other experimental constraints for scalar (top) and fermionic (bottom) dark matter with α_χ conservatively set to 0.5. Both the constraint from data (solid purple) and the expected sensitivity (dashed purple) are shown. The couplings expected for the dark matter relic abundance are also plotted for different values of ε_R in each case.

The result places the strongest constraint on leptophobic dark matter over the entire mass range considered, $2 < m_V < 400$ MeV/c^2, improving the α_B bound by up to two orders of magnitude. Throughout the entire region, the dark-matter relic abundance is excluded for $\varepsilon_R > 0.01$ ($m_V/m_\chi > 2.01$). At the most sensitive mass, $m_V = 80$ MeV/c^2, the scalar result nearly reaches the $\varepsilon_R = 10^{-5}$ line, the most conservative scenario for scalar leptophobic dark matter. This region will be easily accessible with future COHERENT data. This line is excluded for $\alpha_\chi < 0.31$ for $m_V = 80$ MeV/c^2. Though there is no lower bound on the relic abundance in the fermionic case, the data can exclude the model for $\varepsilon_R = 10^{-6}$ ($m_V/m_\chi - 2 \approx 10^{-6}$) for $36 < m_V < 116$ MeV/c^2. This constraint probes a dark matter flux 10000× lower than previous leading constraints, as many of the most sensitive probes of light dark matter are insensitive to leptophobic dark matter. This result was the first performed by a detector sensitive to neutrino-induced CEvNS recoils in a π-DAR and was achieved with a small, 14.6 kg detector. Future data from COHERENT will further probe leptophobic dark matter and can eliminate the model entirely in the scalar scenario with $m_V/m_\chi > 2$.

V. CONCLUSION

COHERENT searched for leptophobic dark-matter particles at the SNS using the full dataset collected by the COHERENT CsI[Na] detector. No dark matter signal was found, and strong constraints on the dark matter model are placed. COHERENT places the most stringent limit to date for all mediator masses $2 < m_V < 400$ MeV/c^2. For scalar dark matter mediated by a 80 MeV/c^2 vector, this result nearly eliminates the studied dark-matter model for $m_V/m_\chi > 2$. Data from future COHERENT CEvNS detectors will strengthen constraints which can fully probe the scalar model and severely limit fermionic, leptophobic dark matter.

ACKNOWLEDGMENTS

The COHERENT collaboration acknowledges the Kavli Institute at the University of Chicago for CsI[Na] detector contributions. The COHERENT collaboration acknowledges the generous resources provided by the ORNL Spallation Neutron Source, a DOE Office of Science User Facility, and thanks Fermilab for the continuing loan of the CENNS-10 detector. We also acknowledge support from the Alfred P. Sloan Foundation, the Consortium for Nonproliferation Enabling Capabilities, the National Science Foundation, the Russian Foundation for Basic Research (proj.# 17-02-01077 A), the Korea National Research

Foundation (NRF 2022R1A3B1078756), and the U.S. Department of Energy, Office of Science. Laboratory Directed Research and Development funds from ORNL and Lawrence Livermore National Laboratory also supported this project. This research used the Oak Ridge Leadership Computing Facility, which is a DOE Office of Science User Facility. The work was supported by the Ministry of Science and Higher Education of the Russian Federation, Project Fundamental properties of elementary particles and cosmology No. 0723-2020-0041.

[1] K. Freese, Int. J. Mod. Phys. **1**, 325 (2017).
[2] E. Aprile *et al.* (XENON Collaboration), Phys. Rev. Lett. **121**, 111302 (2018).
[3] E. Aprile *et al.* (XENON Collaboration), Phys. Rev. Lett. **123**, 251801 (2019).
[4] E. Aprile *et al.* (XENON Collaboration), Phys. Rev. D **103**, 063028 (2021).
[5] A. A. Aguilar-Arevalo *et al.* (MiniBooNE Collaboration), Phys. Rev. Lett. **118**, 221803 (2017).
[6] A. A. Aguilar-Arevalo *et al.*, Phys. Rev. Lett. **129**, 021801 (2022).
[7] B. Lee and S. Weinberg, Phys. Rev. Lett. **39**, 165 (1977).
[8] B. Batell, M. Pospelov, and A. Ritz, Phys. Rev. D **80**, 095024 (2009).
[9] M. Battaglieri *et al.*, arXiv:1707.04591.
[10] D. Akimov *et al.* (COHERENT Collaboration), arXiv:1803.09183.
[11] D. Akimov *et al.* (COHERENT Collaboration), Science **357**, 1123 (2017).
[12] D. Akimov *et al.*, arXiv:2110.07730.
[13] D. Akimov *et al.* (COHERENT Collaboration), arXiv:2110.11453.
[14] D. Akimov *et al.* (COHERENT Collaboration), Phys. Rev. Lett. **126**, 012002 (2021).
[15] D. Akimov *et al.*, J. Instrum. **16**, P08048 (2021).
[16] D. Akimov *et al.* (COHERENT Collaboration), J. Instrum. **17**, P03021 (2022).
[17] D. Akimov *et al.*, arXiv:2204.04575.
[18] A. Aranda and C. D. Carone, Phys. Lett. B **443**, 352 (1998).
[19] P. Gondolo, P. Ko, and Y. Omura, Phys. Rev. D **85**, 035022 (2012).
[20] B. Batell, P. deNiverville, D. McKeen, M. Pospelov, and A. Ritz, Phys. Rev. D **90**, 115014 (2014).
[21] P. deNiverville, M. Pospelov, and A. Ritz, Phys. Rev. D **92**, 095005 (2015).
[22] P. deNiverville, C.-Y. Chen, M. Pospelov, and A. Ritz, Phys. Rev. D **95**, 035006 (2017).
[23] A. Boyarsky, O. Mikulenko, M. Ovchynnikov, and L. Shchutska, J. High Energy Phys. 03 (2022) 006.
[24] E. Cortina Gil *et al.* (NA62 Collaboration), J. High Energy Phys. 05 (2019) 182.
[25] A. A. Aguilar-Arevalo *et al.* (MiniBooNE Collaboration), Phys. Rev. Lett. **118**, 221803 (2017).
[26] A. A. Aguilar-Arevalo *et al.* (MiniBooNE DM Collaboration), Phys. Rev. D **98**, 112004 (2018).
[27] R. Barbieri and T. Ericson, Phys. Lett. **57B**, 270 (1975).
[28] J. A. Dror, R. Lasenby, and M. Pospelov, Phys. Rev. Lett. **119**, 141803 (2017).
[29] J. L. Feng and J. Smolinsky, Phys. Rev. D **96**, 095022 (2017).
[30] B. Dutta, D. Kim, S. Liao, J.-C. Park, S. Shin, L. E. Strigari, and A. Thompson, J. High Energy Phys. 01 (2022) 144.
[31] D. Akimov *et al.* (COHERENT Collaboration), arXiv:2111.02477.
[32] J. I. Collar, N. E. Fields, M. Hai, T. W. Hossbach, J. L. Orrell, C. T. Overman, G. Perumpilly, and B. Scholz, Nucl. Instrum. Methods Phys. Res., Sect. A **773**, 56 (2015).
[33] D. Akimov *et al.* (COHERENT Collaboration), arXiv:2109.11049.
[34] G. J. Feldman and R. D. Cousins, Phys. Rev. D **57**, 3873 (1998).